September 25, 2013

Description of geometric nonlinearity for beam-column analysis in OpenSees

Mark D. Denavit
Stanley D. Lindsey and Associates, Ltd.

Jerome F. Hajjar
Northeastern University

Report No. NEU-CEE-2013-02

Northeastern University was founded in 1898, as a private research university. Northeastern University is a leader in worldwide experiential learning, urban engagement, and interdisciplinary research that meets global and societal needs. Department of Civil and Environmental Engineering has over 100 years of history and tradition in research, teaching and service to the community, making important contributions to the development of our civil infrastructure and the environment, both nationally and internationally.

Contact:

Department of Civil & Environmental Engineering

400 Snell Engineering Center

Northeastern University

360 Huntington Avenue

Boston, MA 02115

(617) 373-2444

(617) 373-4419 (fax)

The work described in this report was conducted as part of a NEESR project supported by the National Science Foundation under Grant No. CMMI-0619047, the American Institute of Steel Construction, the Georgia Institute of Technology, and the University of Illinois at Urbana-Champaign. Any opinions, findings, and conclusions expressed in this material are those of the authors and do not necessarily reflect the views of the National Science Foundation or other sponsors.

Northeastern University

Boston, Massachusetts

September 2013

Abstract

OpenSees is a powerful, object-oriented, open source software framework for simulating the seismic response of structural and geotechnical systems. It has broad capabilities, including geometric nonlinear analysis of frame structures. This report provides a brief description of the formulation for geometric nonlinearity for beam-column elements in OpenSees. The coding structure is described along with the general procedure for state determination. A mathematical description of the various coordinate transformations currently available within the OpenSees framework is presented for two-dimensional elements. Additionally, examples that illustrate the various coordinate transformations are shown.

Introduction

This report is intended to provide a description of geometric nonlinearity for beam-columns in OpenSees. First, the coding structure is described along with the general procedure for state determination. Second, a mathematical description of the various coordinate transformations is presented for two-dimensional elements. Finally, examples which illustrate the various coordinate transformations are shown. For the purposes of this report, elemental loads and nodal offsets have been ignored.

Coding Structure and State Determination

The programming structure of OpenSees allows for independent selection of the beam-column element and geometric transformation. For the standard OpenSees beam-column elements, the difference between geometric linear and geometric nonlinear analysis lies in the geometric transformation alone, since the elements have no internal geometric nonlinearity.

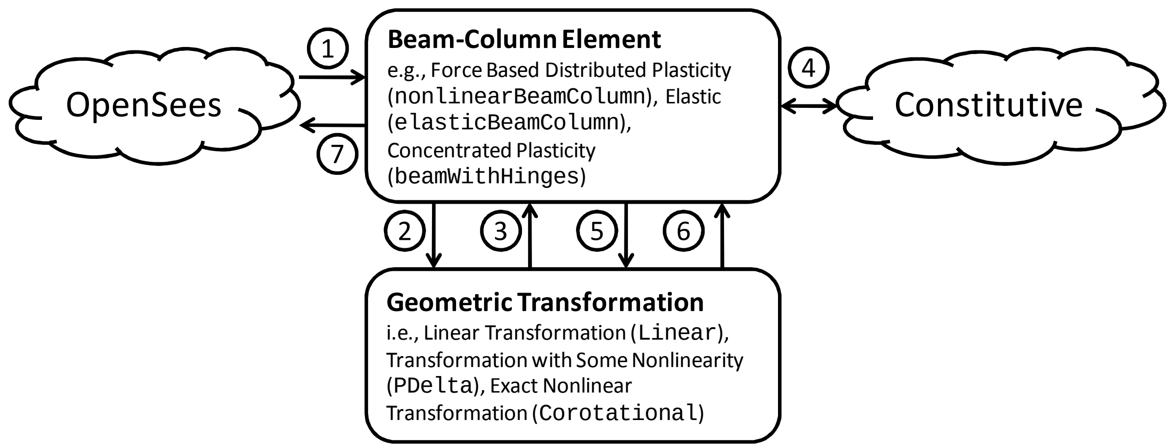

Figure 1. Schematic of Coding Structure

The following is a basic description of the steps involved in the state determination algorithm performed whenever incremental displacements are computed.

1. The element receives global displacements from the connected nodes
2. The element sends the global displacements to the geometric transformation
3. The element receives natural displacements from the geometric transformation
4. The element along with any constitutive relations (sections, etc.) compute element forces and stiffness in the natural coordinates
5. The element sends the element forces and stiffness in the natural coordinates to the geometric transformation
6. The element receives element forces and stiffness in global coordinates from the geometric transformation
7. The element sends (or rather makes available to send upon request) the element forces and stiffness in global coordinates to the analysis

As described in these steps, the main tasks of geometric transformation object are 1) to transform global displacements to natural coordinates and 2) to transform natural forces and stiffnesses to global coordinates. The following section provides a description of how the second task is accomplished for each of the three geometric transformation objects in OpenSees.

Mathematical Description

The transformation can be expressed mathematically through the following equations. The forces in the global system, $\mathbf{Q_{global}}$, are related to the forces in the natural system, $\mathbf{Q_{natural}}$, through the transformation matrix, **T**.

$$\mathbf{Q_{global}} = \mathbf{T}^T \mathbf{Q_{natural}} \qquad [1]$$

The transformation matrix can be separated into two transformations, one that performs the transformation from natural to local coordinates and another that performs the transformation from local to global coordinates.

$$\begin{aligned} \mathbf{T} &= \mathbf{T_{toLocal}} \mathbf{T_{toGlobal}} \\ \mathbf{T}^T &= \mathbf{T}^T_{\mathbf{toGlobal}} \mathbf{T}^T_{\mathbf{toLocal}} \end{aligned} \qquad [2]$$

$$\mathbf{Q_{global}} = \mathbf{T}^T_{\mathbf{toGlobal}} \mathbf{T}^T_{\mathbf{toLocal}} \mathbf{Q_{natural}} \qquad [3]$$

Based on this transformation, the stiffness matrix is also transformed to the global frame through the following relationship noting that the transformation to global coordinates is constant (e.g., Alemdar and White 2005).

$$\begin{aligned} \mathbf{K_{global}} &= \mathbf{T}^T_{\mathbf{toGlobal}} \left(\frac{\partial \mathbf{T}^T_{\mathbf{toLocal}}}{\partial \mathbf{q_{local}}} \mathbf{Q_{natural}} + \mathbf{T}^T_{\mathbf{toLocal}} \mathbf{K_{natural}} \mathbf{T_{toLocal}} \right) \mathbf{T_{toGlobal}} \\ &= \mathbf{T}^T_{\mathbf{toGlobal}} \left(\mathbf{K_{geom,external}} + \mathbf{T}^T_{\mathbf{toLocal}} \mathbf{K_{natural}} \mathbf{T_{toLocal}} \right) \mathbf{T_{toGlobal}} \end{aligned} \qquad [4]$$

In two dimensions, with force vectors defined as in Equations 5 and 6, the exact transformation matrix is shown in Equation 7, where β is the angle between the positive x axis and the element and L is the length of the element as shown in Figure 2. It should be noted that with an exact transformation, the values used for β and L are current rather than initial. This transformation is used by the `Corotational` transformation in OpenSees.

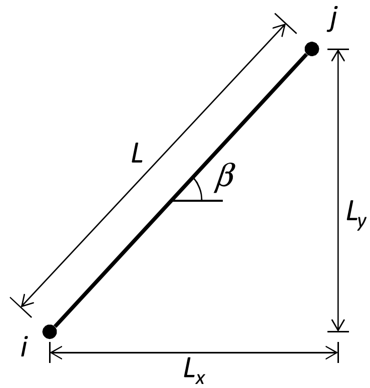

Figure 2. Geometry of a beam-column element

$$\mathbf{Q}^T_{\mathbf{natural}} = \left\{ P \quad M_i \quad M_j \right\} \tag{5}$$

$$\mathbf{Q}^T_{\mathbf{global}} = \left\{ F_{xi} \quad F_{yi} \quad M_i \quad F_{xj} \quad F_{yj} \quad M_j \right\} \tag{6}$$

$$\mathbf{T} = \begin{bmatrix} -\cos\beta & -\sin\beta & 0 & \cos\beta & \sin\beta & 0 \\ -\dfrac{\sin\beta}{L} & \dfrac{\cos\beta}{L} & 1 & \dfrac{\sin\beta}{L} & -\dfrac{\cos\beta}{L} & 0 \\ -\dfrac{\sin\beta}{L} & \dfrac{\cos\beta}{L} & 0 & \dfrac{\sin\beta}{L} & -\dfrac{\cos\beta}{L} & 1 \end{bmatrix} \tag{7}$$

$$\mathbf{T}_{\mathbf{toGlobal}} = \begin{bmatrix} \cos\beta & \sin\beta & 0 & 0 & 0 & 0 \\ -\sin\beta & \cos\beta & 0 & 0 & 0 & 0 \\ 0 & 0 & 1 & 0 & 0 & 0 \\ 0 & 0 & 0 & \cos\beta & \sin\beta & 0 \\ 0 & 0 & 0 & -\sin\beta & \cos\beta & 0 \\ 0 & 0 & 0 & 0 & 0 & 1 \end{bmatrix} \tag{8}$$

$$\mathbf{T}_{\mathbf{toLocal}} = \begin{bmatrix} -1 & 0 & 0 & 1 & 0 & 0 \\ 0 & 1/L & 1 & 0 & -1/L & 0 \\ 0 & 1/L & 0 & 0 & 1/L & 1 \end{bmatrix} \tag{9}$$

The resulting external geometric stiffness matrix is shown in Equation 10.

$$\mathbf{K}_{\mathbf{geom,external}} = \frac{P}{L}\begin{bmatrix} ss & -cs & 0 & -ss & cs & 0 \\ -cs & cc & 0 & cs & -cc & 0 \\ 0 & 0 & 0 & 0 & 0 & 0 \\ -ss & cs & 0 & ss & -cs & 0 \\ cs & -cc & 0 & -cs & cc & 0 \\ 0 & 0 & 0 & 0 & 0 & 0 \end{bmatrix} + \frac{M_1+M_2}{L^2}\begin{bmatrix} -2cs & cc-ss & 0 & 2cs & -cc+ss & 0 \\ cc-ss & 2cs & 0 & -cc+ss & -2cs & 0 \\ 0 & 0 & 0 & 0 & 0 & 0 \\ 2cs & -cc+ss & 0 & -2cs & cc-ss & 0 \\ -cc+ss & -2cs & 0 & cc-ss & 2cs & 0 \\ 0 & 0 & 0 & 0 & 0 & 0 \end{bmatrix} \qquad [10]$$

where, $c = \cos\alpha$, $s = \sin\alpha$, and α is the rotation of the displaced chord from the initial chord

For the `Linear` coordinate transformation, the transformation matrices take the form shown in Equations 11 and 12, where the subscript "$_o$" indicates the initial value. These matrices are identical those of the exact transformation (Equations 8 and 9) with the exception that initial values are used for the orientation and length of the element, resulting in a constant transformation matrix. Since the transformation matrix is constant the external geometric stiffness matrix is zero (Equation 13).

$$\mathbf{T}_{\mathbf{toGlobal}} = \begin{bmatrix} \cos\beta_o & \sin\beta_o & 0 & 0 & 0 & 0 \\ -\sin\beta_o & \cos\beta_o & 0 & 0 & 0 & 0 \\ 0 & 0 & 1 & 0 & 0 & 0 \\ 0 & 0 & 0 & \cos\beta_o & \sin\beta_o & 0 \\ 0 & 0 & 0 & -\sin\beta_o & \cos\beta_o & 0 \\ 0 & 0 & 0 & 0 & 0 & 1 \end{bmatrix} \qquad [11]$$

$$\mathbf{T}_{\mathbf{toLocal}} = \begin{bmatrix} -1 & 0 & 0 & 1 & 0 & 0 \\ 0 & 1/L_o & 1 & 0 & -1/L_o & 0 \\ 0 & 1/L_o & 0 & 0 & 1/L_o & 1 \end{bmatrix} \qquad [12]$$

$$\mathbf{K}_{\mathbf{geom,external}} = \mathbf{0} \qquad [13]$$

For the `PDelta` coordinate transformation, the transformation matrices take the form shown in Equations 15 and 16, where $\delta\Delta_y$ is the difference between transverse displacements at the nodes in local coordinates (Equation 14). The additional terms in Equation 16 (as compared to Equation 12) are the "P-Delta" terms and make the transformation not constant, resulting in an external geometric stiffness matrix (Equation 17)

$$\delta\Delta_y = \Delta_{y,node\,i} - \Delta_{y,node\,j} \qquad [14]$$

$$\mathbf{T}_{\mathbf{toGlobal}} = \begin{bmatrix} \cos\beta_o & \sin\beta_o & 0 & 0 & 0 & 0 \\ -\sin\beta_o & \cos\beta_o & 0 & 0 & 0 & 0 \\ 0 & 0 & 1 & 0 & 0 & 0 \\ 0 & 0 & 0 & \cos\beta_o & \sin\beta_o & 0 \\ 0 & 0 & 0 & -\sin\beta_o & \cos\beta_o & 0 \\ 0 & 0 & 0 & 0 & 0 & 1 \end{bmatrix} \qquad [15]$$

$$\mathbf{T}_{\mathbf{toLocal}} = \begin{bmatrix} -1 & {}^{\delta\Delta_y}/_{L_o} & 0 & 1 & -{}^{\delta\Delta_y}/_{L_o} & 0 \\ 0 & {}^{1}/_{L_o} & 1 & 0 & -{}^{1}/_{L_o} & 0 \\ 0 & {}^{1}/_{L_o} & 0 & 0 & {}^{1}/_{L_o} & 1 \end{bmatrix} \qquad [16]$$

$$\mathbf{K}_{\mathbf{geom,external}} = \begin{bmatrix} 0 & 0 & 0 & 0 & 0 & 0 \\ 0 & {}^{P}/_{L_o} & 0 & 0 & -{}^{P}/_{L_o} & 0 \\ 0 & 0 & 0 & 0 & 0 & 0 \\ 0 & 0 & 0 & 0 & 0 & 0 \\ 0 & -{}^{P}/_{L_o} & 0 & 0 & {}^{P}/_{L_o} & 0 \\ 0 & 0 & 0 & 0 & 0 & 0 \end{bmatrix} \qquad [17]$$

Example Analyses

Euler Buckling of a Simply Supported Column

The ability of the three coordinate transformations to detect the Euler buckling load is studied by analyzing a simply supported column (Figure 3a). The column is without imperfection and the load is applied concentrically. The critical load of the column is given analytically by Equation 18, assuming an effective length factor, *K*, of 1.

$$P_{cr} = \frac{\pi^2 EI}{(KL)^2} \qquad [18]$$

In the analysis, the critical load is the load at which the minimum Eigen value of the stiffness matrix becomes zero. The analyses were performed with one to five displacement-based elastic beam-column elements (`elasticBeamColumn`) along the height of the column.

The computational results and error statistics are shown in Figure 3c. From this data several observations can be made:

- The lack of a critical load when only one element is used confirms that no P-δ geometric nonlinearity is implemented within the element.
- The lack of P-δ geometric nonlinearity implemented within the element results in a much slower convergence to theoretical results. As a point of comparison, an element with internal geometric stiffness can obtain results within 1% with two elements and within 0.1% with four elements (Denavit and Hajjar 2010).
- The difference between the `Corotational` and `PDelta` transformations is small.
- The analyses with the `Linear` transformation, as expected, did not exhibit a critical load.

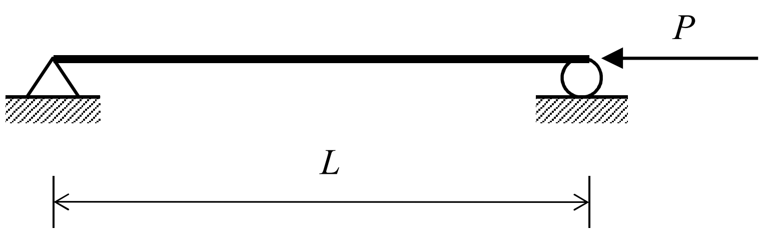

(a) Configuration

$E = 29{,}000$
$I = 110$
$A = 9.12\times10^3$
$L = 60$
$P_{cr} = 8{,}745.6$

(b) Properties

Number of Elements	Corotational Critical Load	Corotational Percent Error	PDelta Critical Load	PDelta Percent Error	Linear Critical Load	Linear Percent Error
1	∞	∞	∞	∞	∞	∞
2	10,634	21.59%	10,633	21.58%	∞	∞
3	9,570.3	9.43%	9,570.0	9.43%	∞	∞
4	9,204.0	5.24%	9,203.7	5.24%	∞	∞
5	9,037.2	3.33%	9,036.9	3.33%	∞	∞
10	8,818.0	0.83%	8,817.7	0.82%	∞	∞
30	8,753.9	0.10%	8,753.6	0.09%	∞	∞
100	8,746.6	0.01%	8,746.3	0.01%	∞	∞

(c) Results

Figure 3. Configuration and Results of the Analysis of a Simply Supported Beam under Axial Loading

Cantilever under Axial Loading

To compare the behavior of the three different coordinate transformations, the response of a cantilever column under axial loading is studied. The structure, as described in Figure 4a, is initially straight. A small bending moment is applied at the free end to introduce a perturbation.

Analyses are performed with 5 elastic displacement-based beam-column elements (`elasticBeamColumn`) along the height of the column. The analysis results are compared to the analytical solution given in Southwell (1941).

The results (Figure 4c) show a wide variety of behavior. As expected the `Linear` transformation produced a linear load-deformation response and constant Eigen value. The `Corotational` transformation follows very closely the analytical solution to very high levels of load and deformation. The `PDelta` transformation produces similar results to that of the `Corotational` transformation up to a load near the critical load. However, near the critical load, the deformation increases asymptotically and above the critical load the deformation is in the opposite direction of the analytical solution. This analysis indicates that for low to medium levels of axial load, the `PDelta` transformation will provide accurate results but for high levels the results may be very inaccurate.

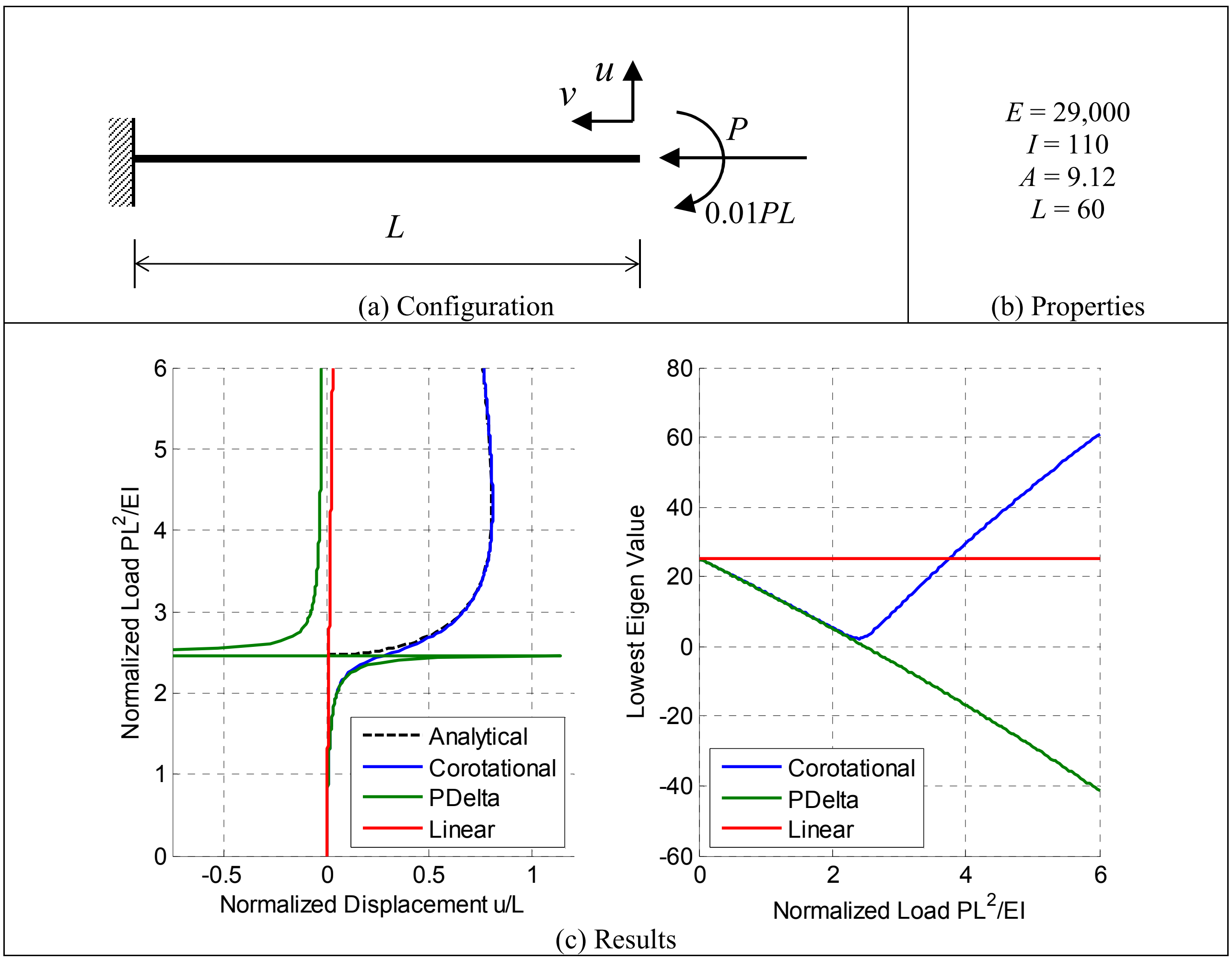

Figure 4. Configuration and Results of the Analysis of a Cantilever under Axial Loading

Cantilever under Axial and Transverse Loading

To study the accuracy of the two nonlinear coordinate transformations in a more practical sense, the response of a cantilever column under axial and transverse loading is studied. The structure, as described in Figure 5a, is initially straight. Analyses are performed for both strong and weak axis bending with varying number of elastic displacement-based beam-column elements (`elasticBeamColumn`) distributed uniformly along the height of the column. The analysis results are compared to the analytical solution given in Equations 19 through 21 (AISC 2005).

$$M_{MAX}\left(@\,x=0\right)=HL\left(\frac{\tan\alpha}{\alpha}\right) \qquad [19]$$

$$y_{MAX}\left(@\,x=L\right)=\frac{HL^3}{3EI}\left(\frac{3\left(\tan\alpha-\alpha\right)}{\alpha^3}\right) \qquad [20]$$

$$\alpha=\sqrt{\frac{PL^2}{EI}} \qquad [21]$$

The computational results and error statistics are shown in Figure 5c and d. From this data several observations can be made:

- The accuracy of the deformation results is lower than that of the moment results.
- The accuracy of the weak axis bending results is lower than that of the strong axis bending results. This can be attributed to greater nonlinearity in the weak axis bending case. The greater nonlinearity is due to the greater slenderness in the weak axis and is seen in the ratio between exact and first order results.
- Multiple elements along the length of the member are necessary to ensure accuracy of results. In the case of strong axis bending, 2 elements is likely appropriate while in the case of weak axis bending, 4 elements is likely appropriate.

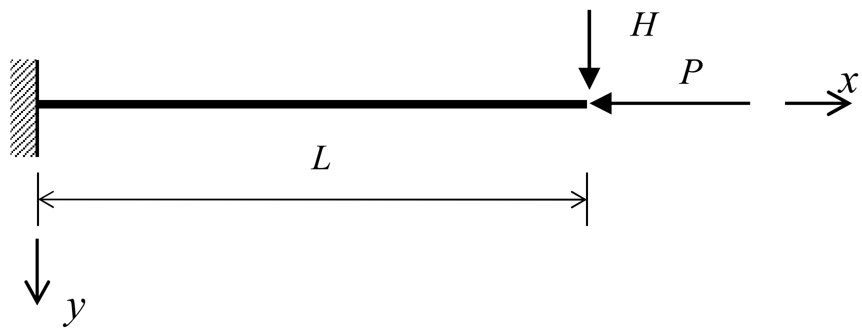

(a) Configuration

$E = 29{,}000$
$I_{strong} = 110$
$I_{weak} = 37.1$
$A = 9.12$
$L = 180$
$P = 50$
$H = 1$

(b) Properties

Number of Elements	PDelta M_{MAX}	PDelta % Error	PDelta y_{MAX}	PDelta % Error	Corotational M_{MAX}	Corotational % Error	Corotational y_{MAX}	Corotational % Error
1	216.7	-0.73%	0.734	-4.14%	216.6	-0.75%	0.733	-4.18%
2	217.8	-0.22%	0.756	-1.25%	217.7	-0.24%	0.755	-1.30%
3	218.0	-0.10%	0.761	-0.58%	218.0	-0.12%	0.760	-0.62%
4	218.1	-0.06%	0.763	-0.33%	218.1	-0.08%	0.762	-0.37%
6	218.2	-0.03%	0.764	-0.15%	218.2	-0.05%	0.764	-0.19%
First Order	180.0		0.609		180.0		0.609	
Exact	218.3		0.765		218.3		0.765	

(c) Strong Axis Bending Results

Number of Elements	PDelta M_{MAX}	PDelta % Error	PDelta y_{MAX}	PDelta % Error	Corotational M_{MAX}	Corotational % Error	Corotational y_{MAX}	Corotational % Error
1	361.4	-11.82%	3.628	-21.08%	361.1	-11.88%	3.624	-21.15%
2	393.4	-4.02%	4.267	-7.16%	393.0	-4.11%	4.261	-7.29%
3	402.0	-1.90%	4.441	-3.39%	401.6	-2.01%	4.434	-3.54%
4	405.4	-1.09%	4.507	-1.95%	404.9	-1.20%	4.500	-2.10%
6	407.8	-0.49%	4.556	-0.88%	407.3	-0.61%	4.549	-1.04%
8	408.7	-0.28%	4.574	-0.50%	408.2	-0.40%	4.566	-0.66%
10	409.1	-0.18%	4.582	-0.32%	408.6	-0.30%	4.574	-0.48%
First Order	180.0		1.807		180.0		1.807	
Exact	409.8		4.597		409.8		4.597	

(d) Weak Axis Bending Results

Figure 5. Configuration and Results of the Analysis of a Cantilever under Axial and Transverse Loading

Simply Supported Column with End Moments

In some cases the critical moment is not at a member end to investigate this, the response of a simply supported column with end moments is studied. The structure, as described in Figure 6a, is initially straight. Analyses are performed with varying number of elastic displacement-based beam-column elements (`elasticBeamColumn`) distributed uniformly along the length of the column. The load is a fraction of P_{e1} which is computed using Equation 22. The analysis results are compared to converged results obtained using a large number of elements.

$$P_{e1} = \frac{\pi^2 EI}{L^2} \qquad [22]$$

Nodal displacements and bending moments are shown in Figure 6c for analyses with one, two, and three elements as well as converged results. The computational results and error statistics are tabulated in Figure 6d. From this data several observations can be made:

- The maximum moment does not occur at a member end due the P-δ effect.
- With one element, since the P-δ effect is not modeled, no nonlinearity is detected and the results are the same as that of a first order analysis.
- There is not a monotonic increase in accuracy with increase in elements. This is because the maximum moment and displacement no not necessarily occur at element ends where these values are monitored. More accurate results are attained if element ends happen to be near the location of the maximum value. It should be noted that the maximum of the nodal displacements is taken as the maximum displacement, a more accurate method for determining the maximum displacement from an analysis would utilize the cubic displacement shape functions.
- Multiple elements along the length of the member are necessary to ensure accuracy of results. Three elements appear to be appropriate for attaining accurate bending moments, while, six elements appear to be appropriate for attaining accurate transverse displacements.

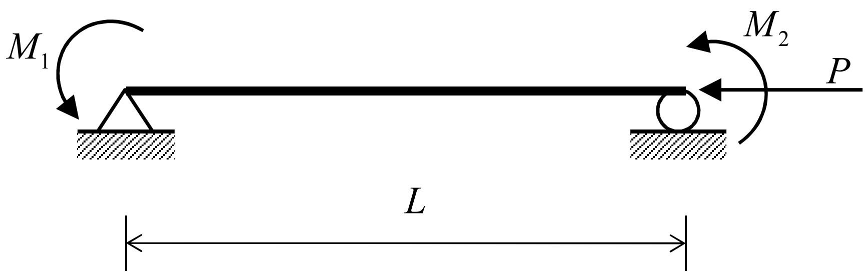

(a) Configuration

$E = 29{,}000$
$I = 110$
$A = 9.12$
$L = 120$
$P = 0.3P_{e1}$
$M_1 = 12P$
$M_2 = -M_1/2$

(b) Properties

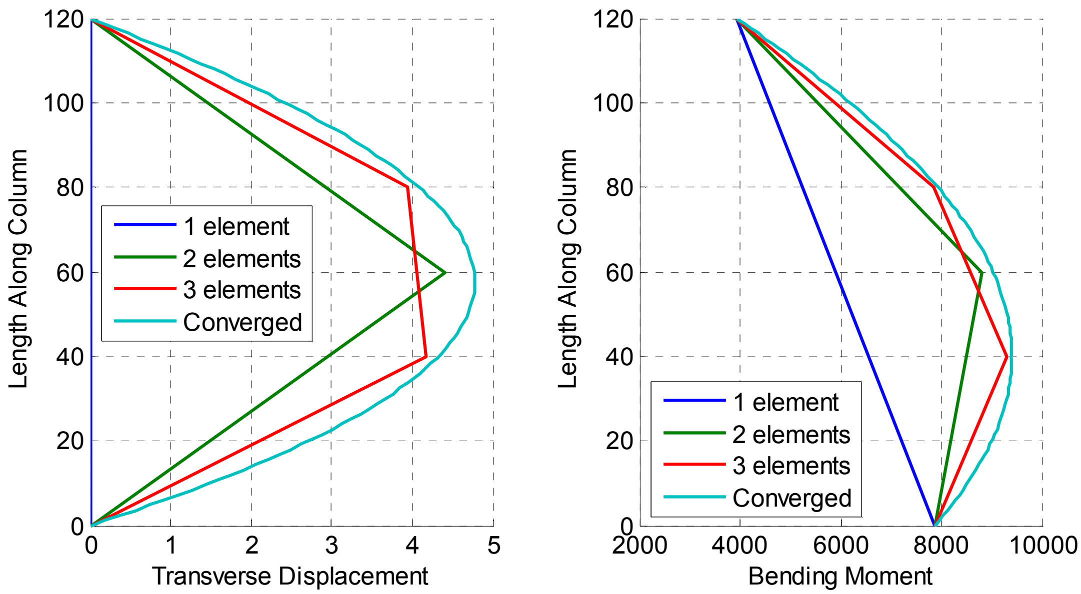

(c) Results

Number of Elements	PDelta M_{MAX}	% Error	y_{MAX}	% Error	Corotational M_{MAX}	% Error	y_{MAX}	% Error
1	7,871	-16.27%	0.000	-100.00%	7,871	-16.27%	0.000	-100.00%
2	8,804	-6.35%	4.422	-7.43%	8,791	-6.48%	4.402	-7.85%
3	9,311	-0.95%	4.195	-12.18%	9,298	-1.09%	4.172	-12.68%
4	9,259	-1.51%	4.697	-1.68%	9,247	-1.63%	4.669	-2.26%
5	9,320	-0.85%	4.609	-3.51%	9,304	-1.03%	4.581	-4.10%
6	9,389	-0.12%	4.754	-0.49%	9,374	-0.28%	4.724	-1.11%
10	9,387	-0.14%	4.783	0.13%	9,373	-0.29%	4.753	-0.51%
Converged	9,400		4.777		9,400		4.777	

(d) Tabular Results

Figure 6. Configuration and Results of the Analysis of a Simply Supported Column with End Moments

References

Alemdar, B. N. and White, D. W. (2005). "Displacement, Flexibility, and Mixed Beam-Column Finite Element Formulations for Distributed Plasticity Analysis," *Journal of Structural Engineering*, ASCE, 131(12), 1811-1819.

American Institute of Steel Construction (AISC) (2005). ANSI/AISC360-05: *Specification for Structural Steel Buildings*, AISC, Chicago, Illinois.

Denavit, M. D. and Hajjar, J. F. (2010). "Nonlinear Seismic Analysis of Circular Concrete-Filled Steel Tube Members and Frames," Report No. NSEL-023, Newmark Structural Laboratory Report Series (ISSN 1940-9826), Department of Civil and Environmental Engineering, University of Illinois at Urbana-Champaign, Urbana, Illinois, March.

OpenSees (2013). "Open System for Earthquake Engineering Simulation," Open source software, http://opensees.berkeley.edu.

Southwell, R. V. (1941). *Introduction to the Theory of Elasticity for Engineers and Physicists*, Oxford University Press.

Department of Civil and Environmental Engineering Reports

Northeastern University

REPORT NO.	AUTHORS	TITLE	DATE
NEU-CEE-2013-02	Denavit, M. D.; Hajjar, J. F.	Description of Geometric Nonlinearity for Beam-Column Analysis in OpenSees	September 2013
NEU-CEE-2013-01	Hajjar, J. F.; Sesen, A. H.; Jampole, E.; Wetherbee, A.	A Synopsis of Sustainable Structural Systems with Rocking, Self-Centering, and Articulated Energy-Dissipating Fuses	June 2013
NEU-CEE-2011-01	Hajjar, J. F.; Guldur, B.; and Sesen, A. H.	Laboratory for Structural Testing of Resilient and Sustainable Systems (STReSS Laboratory)	September 2011